Effects of Non-local Scattering on the Aerodynamic Coefficients of Nanosized Particles

Aldo Frezzotti, Marco Carnini
Dipartimento di Matematica, Politecnico di Milano, Italy
E-mail: aldo.frezzotti@polimi.it, marco.carnini@polimi.it

Keywords: Kinetic theory, Gas-surface interaction, Nano-particles.

SUMMARY. Most gas-surface interaction models used in rarefied gas dynamics assume that the space and time scale associated with gas-solid interaction are negligibly small. Accordingly, it is assumed that a gas molecule hitting a solid surface is *instantaneously* re-emitted at the *same* spatial location. However, as shown by molecular dynamics simulation, the re-emission event usually takes place at a distance of several molecular diameters from the first collision location. It is to expected that diffusion processes on the surface do affect the aerodynamic forces on particles transported by a carrier gas, when the particle size is comparable with the distance covered by a molecule on the solid surface during interaction. In such case, local gas-surface interaction models fail to predict the correct drag on the particle. In this paper a non-local kinetic gas-surface interaction model is applied to compute aerodynamic forces on spherical particles in the free molecular flow regime. Is is shown that effective accommodation coefficients of nanosized particles depend on particle radius.

1 INTRODUCTION

Transport properties of nanoparticles carried by a rarefied gas play an important role in many processes: aerosols dynamics[1], nanostructure manufacturing[2] and health protection. In principle, the aerodynamic forces acting on a solid body moving through a dilute gas can be computed from the Boltzmann equation[3], provided a suitable gas-surface interaction model is specified to describe collisions between carrier gas and solid body molecules. In the vast majority of rarefied gas dynamics applications, gas-surface interaction is described by assigning the boundary condition for the gas distribution function $f(\boldsymbol{r}, \boldsymbol{v}|t)$ at the points of the solid body surface:

$$(\boldsymbol{v}\circ\boldsymbol{n})f(\boldsymbol{r},\boldsymbol{v}|t) = \int_{\boldsymbol{v}_1\circ\boldsymbol{n}<0} K_w(\boldsymbol{v}_1\rightarrow\boldsymbol{v})|\boldsymbol{v}_1\circ\boldsymbol{n}|f(\boldsymbol{r},\boldsymbol{v}_1|t)\,d\boldsymbol{v}_1 \qquad \boldsymbol{v}\circ\boldsymbol{n}>0 \tag{1}$$

Eq.(1) relates the flux of atoms re-emitted with velocity $\boldsymbol{v}$ at a location $\boldsymbol{r}$ on the surface to the flux of atoms impinging on the surface. The linearity of the relationships stems from the assumption that the impinging atomic flux does not affects the physical state of the surface. In particular, $\boldsymbol{n}$ is a unit vector normal to the wall surface and directed towards the fluid region whereas $K_w(\boldsymbol{v}_1 \rightarrow \boldsymbol{v})$ is a scattering kernel which gives the probability that a molecule impinging on the wall with velocity between $\boldsymbol{v}_1$ and $\boldsymbol{v}_1 + d\boldsymbol{v}_1$ is *instantaneously* re-emitted at the *same location* $\boldsymbol{r}$ with velocity between $\boldsymbol{v}$ and $\boldsymbol{v} + d\boldsymbol{v}$. Since the rigorous determination of $K_w(\boldsymbol{v}_1 \rightarrow \boldsymbol{v})$ would require the determination of the complex dynamics of a fluid molecule in interaction with wall molecules, scattering kernel expressions are derived from phenomenological models[3]. Maxwell's model is the most widely used choice for $K_w(\boldsymbol{v}_1 \rightarrow \boldsymbol{v})$ which takes the form:

$$\begin{aligned} K_w(\boldsymbol{v}_1\rightarrow\boldsymbol{v}) &= \alpha(\boldsymbol{v}\circ\boldsymbol{n})\frac{1}{2\pi(RT_w)^2}\exp\left(-\frac{\boldsymbol{v}^2}{2RT_w}\right) + \\ &\quad (1-\alpha)\delta(\boldsymbol{v}-\boldsymbol{v}_1+2(\boldsymbol{v}_1\circ\boldsymbol{n})\boldsymbol{n}), \qquad 0\le\alpha\le 1 \end{aligned} \tag{2}$$

In Eq.(2) T_w is the wall temperature, whereas the coefficient α is, at the same time, the probability of diffuse re-emission and the value of the accommodation coefficient of any molecular property $\psi(\boldsymbol{v})$ which is an even function of $\boldsymbol{v} \circ \boldsymbol{n}$[3]. As is clear from Eq. (2), Maxwell's model simply assumes that an atom impinging on the wall has a probability α of being completely thermalized and a probability $1 - \alpha$ of being specularly reflected. Boundary conditions in the form given by Eq.(1) assume that the solid is represented by a well defined, structurless and impenetrable surface. Moreover, it is assumed that both the time a gas molecule spends interacting with the solid and the displacement, caused by diffusion processes on the surface, are much smaller than the characteristic gasdynamic time and space scales. Accordingly, the scattering kernel in Eq.(1) simply relates (in a probabilistic sense) the molecular velocities before and after interaction with the solid, re-emission being instantaneous and local. Although adequate to deal with rarefied gas flow around macroscopic bodies, the model described above is expected to fail when applied to compute interactions between a carrier gas and a cluster whose radius amounts to a few molecular diameters. As a matter of fact, all of the assumptions at the base of Eq.(1) are no longer valid, in this case. First of all, as discussed by Tammet[4], nanoparticles cannot be given a precisely defined geometrical collision radius. Actually, the collective effects of gas-solid attractive intermolecular forces are felt in a layer which surrounds the nominal particle surface, determined by short range repulsive forces. The layer thickness is of the order of a few molecular diameters but its effective size depends on the relative velocity of a gas molecule approaching the nanoparticle[4]. Such layer obviously surrounds bodies of any size, but its presence only plays a role when the particle size is comparable to the layer thickness. As mentioned above, the traditional approach neglects surface diffusion processes which cause gas molecules to be desorbed from the solid surface a few molecular diameters away from the absorption position. Again, surface diffusion has a negligible effect on macroscopic bodies, but might affect aerodynamic forces on nanosized particles. In Refs.[4] and [5] phenomenological models are proposed to take into account some of the nanoparticles peculiarities mentioned above. It has also been argued that momentum accommodation might be affected by particle radius, being smaller for nanosized particles[5] as also suggested by an experimental investigation[6]. In order to provide firmer theoretical support to the conjecture, Li and Wang[7] performed a number of molecular dynamics (MD) simulations of single gas molecule scattering from a small cluster. Indirect evidence of drag reduction has been reported, however no evaluation of aerodynamic forces is given. Although MD simulations are perfectly adequate to obtain aerodynamic forces, the computational cost of the technique might be prohibitive. As shown below, estimating drag coefficients with 1% accuracy requires generating about 10^6 independent trajectories, each of them requiring the calculation of the motion of the gas molecule and the few hundreds/thousands molecules forming the cluster.

The aim of the present paper is to show that the limitations of the local scattering kernel model and high computational cost of MD simulations can be overcome by a kinetic model[8] based on a simplified dynamics of a gas molecule interacting with the solid wall. The model uses the same physical quantities (interaction potentials, molecular masses...) MD simulations are based on, however the expensive multibody dynamics computation is avoided by introducing an assumption on pair correlations. The simplified correlation model leads to a closed kinetic equation for the one-particle gas distribution function. The structure of the kinetic equation is not simple but it can be solved numerically by a stochastic particle scheme[9] which computes several thousands of trajectories per second on a personal computer. Hence, the numerical computation of aerodynamic forces can be accomplished in a few minutes with good accuracy. Comparisons of kinetic model and MD predictions has been carried out in Refs.[8] and [10] where it is shown that it is possible to reproduce the results of MD simulations with a degree of accuracy good enough to capture the behavior of

aerodynamic forces on nanoparticles to be examined in the present study. The remaining part of the paper is organized as follows: section 2 provides a concise description of the kinetic model; the application to the computation of drag coefficients on spherical nanoparticle is described in section 3; finally, section 4 briefly summarizes the obtained results.

2 MATHEMATICAL MODEL DESCRIPTION

Following Ref. [8], we consider a system composed by a monatomic fluid interacting with solid walls. Fluid molecules have mass m_1 and nominal diameter σ_1, whereas m_2 and σ_2 are the mass and nominal diameter of wall molecules, respectively. Fluid-wall interaction forces are obtained from the potentials $\phi^{(12)}(\rho)$ given by the following expressions:

$$\phi^{(12)}(\rho) = \begin{cases} +\infty & \rho < \sigma_{12} \\ -\overline{\phi}^{(12)} \left(\frac{\rho}{\sigma_{12}}\right)^{-\gamma^{(12)}} & \rho \geq \sigma_{12} \end{cases} \tag{3}$$

As shown above, $\phi^{(12)}$ is obtained by superposing a soft tail to hard sphere potential determined by the hard sphere diameter $\sigma_{12} = (\sigma_1 + \sigma_2)/2$. The adoption of simplifying assumptions about pair correlations [8] allows the derivation of the following kinetic equation for the one-particle distribution function $f(\boldsymbol{r}, \boldsymbol{v}|t)$ of fluid molecules:

$$\frac{\partial f}{\partial t} + \boldsymbol{v} \circ \frac{\partial f}{\partial \boldsymbol{r}} + \frac{\boldsymbol{F}(\boldsymbol{r}|t)}{m_1} \circ \frac{\partial f}{\partial \boldsymbol{v}} = C^{(12)}(f_w, f) \tag{4}$$

The term $C^{(12)}(f_w, f)$ represents the hard sphere collision integral defined by the expression

$$C^{(12)}(f_w, f) = \sigma_{12}^2 \int \Big\{ \chi^{(12)}(\boldsymbol{r}, \boldsymbol{r} + \sigma_{12}\hat{\boldsymbol{k}}) f_w(\boldsymbol{r} + \sigma_{12}\hat{\boldsymbol{k}}, \boldsymbol{v}_1^*|t) f(\boldsymbol{r}, \boldsymbol{v}^*|t) - \chi^{(12)}(\boldsymbol{r}, \boldsymbol{r} - \sigma_{12}\hat{\boldsymbol{k}}) f_w(\boldsymbol{r} - \sigma_{12}\hat{\boldsymbol{k}}, \boldsymbol{v}_1|t) f(\boldsymbol{r}, \boldsymbol{v}|t) \Big\} (\boldsymbol{v}_r \circ \hat{\boldsymbol{k}})^+ d\boldsymbol{v}_1 d^2\hat{\boldsymbol{k}} \tag{5}$$

where f_w is the distribution function of wall molecules whereas $\chi^{(12)}$ is the contact value of the gas-solid pair correlation function. The self-consistent force field $\boldsymbol{F}^{(12)}(\boldsymbol{r})$ is defined as

$$\boldsymbol{F}^{(12)}(\boldsymbol{r}) = \int_{\|\boldsymbol{r}_1 - \boldsymbol{r}\| > \sigma_{12}} \frac{d\phi^{(12)}}{d\rho} \frac{\boldsymbol{r}_1 - \boldsymbol{r}}{\|\boldsymbol{r}_1 - \boldsymbol{r}\|} n_w(\boldsymbol{r}_1)\, d\boldsymbol{r}_1 \tag{6}$$

In absence of long range spatial correlations, $\boldsymbol{F}^{(12)}(\boldsymbol{r})$ is a linear functional of the wall number density $n_w(\boldsymbol{r})$. It is worth stressing that, in the framework of the present model, fluid-wall interaction is not present in the form of a boundary condition, but it is taken into account through an explicit, although approximate, microscopic model. In particular, it is assumed that the motion of a gas atom in the vicinity of the wall is determined by the stationary force field $\boldsymbol{F}^{(12)}(\boldsymbol{r})$ generated by the long range potential tails of wall atoms, when the distance ρ exceeds σ_{12}. At shorter distances, the effect of intense repulsive forces is added by the collision integral $C^{(12)}(f, f_w)$ which describes binary elastic collisions between gas and wall molecules. It is therefore assumed that repulsion on a gas molecule is caused just by the closest wall molecule. However, the collective effect of nearby wall molecules on the frequency of binary encounters is felt through $\chi^{(12)}$. Although no explicit assumption is made about the interaction among wall atoms, it is assumed that walls are in

a prescribed state of equilibrium which is not altered by the interaction with the gas phase. Hence, the velocity distribution function f_w will take the following form

$$f_w(\boldsymbol{r},\boldsymbol{v}) = \frac{n_w(\boldsymbol{r})}{(2\pi R_2 T_w(\boldsymbol{r}))^{3/2}} \exp\left\{-\frac{[\boldsymbol{v}-\boldsymbol{u}_w(\boldsymbol{r})]^2}{2R_2 T_w(\boldsymbol{r})}\right\} \tag{7}$$

being $n_w(\boldsymbol{r})$, $T_w(\boldsymbol{r})$ and $\boldsymbol{u}_w(\boldsymbol{r})$ the wall atoms number density, temperature and mean velocity, respectively. The gas constant R_2 is defined as $\frac{k_B}{m_2}$, where k_B is the Boltzmann constant. The specific form of $\chi^{(12)}(n_w)$ is taken from an approximate expression for the contact value of the pair correlation function of a single component hard sphere gas in uniform equilibrium [11]:

$$\chi^{(12)}(n_w) = \frac{1}{2}\frac{2-\eta_{12}}{(1-\eta_{12})^3}, \qquad \eta_{12} = \frac{\pi}{6} n_w \sigma_{12}^3 \tag{8}$$

where η_{12} is the volume fraction occupied by hard sphere cores. Eq. (8) provides a very accurate approximation of the contact value of the uniform equilibrium pair correlation function in a single component hard sphere gas, but its use in the present context is questionable. However, the physical consequences of the above assumption are quite reasonable. Actually, it is easily shown that, in the presence of a wall density gradient, the hard sphere term produces a net repulsive force proportional to $\chi^{(12)}(n_w)$ in the vicinity of the wall surface [8].

3 AERODYNAMIC FORCES ON NANOSIZED PARTICLES IN THE FREE MOLECULAR FLOW REGIME

The kinetic model described in the previous section has been adopted to study the free molecular flow of Xenon gas past a Platinum sphere and obtain the drag coefficient C_D as a function of the downstream gas Mach number and sphere radius. This particular choice has been simply dictated by the availability of previous results on the $Xe-Pt$ system [8, 10] which, although obtained in different flow geometries, are relevant for the analysis of the present problem. Inspection of Eqs.(4,5) easily shows that, if T_{ref} is a reference temperature value, then the three quantities σ_1, $\sigma_1/\sqrt{\frac{k_B T_{ref}}{m_1}}$ and m_1 can be adopted as units for length, time and mass, respectively. The gas-surface interaction model is then characterized by the following dimensionless parameters: σ_{12}/σ_1, $\overline{\phi}^{(12)}/k_B T_{ref}$, $\gamma^{(12)}$, m_2/m_1 and $\eta_w = \frac{\pi \overline{n}_w {\sigma_1}^3}{6}$. The nature and number of additional parameters depend on the problem at hand. In the computations described below the reference temperature T_{ref} has been set equal to $300^o K$, the ratio σ_{12}/σ_1 has been set equal to one, the normalized depth of the potential well, $\overline{\phi}^{(12)}/k_B T_{ref}$, has been set equal to $\gamma^{(12)} = 6$ to match the attractive tail of the Lennard-Jones potential, the mass ratio m_2/m_1 has been set equal to 1.486 and the solid reduced density η_w has been set equal to 0.7, a reasonable choice for solid Pt at the reference temperature. Although η_{12} is completely specified by the parameters listed above, the strength of the repulsive effects of hard sphere collisions at walls has been tuned by varying η_{12} as if it were an independent parameter, slightly forcing the model structure. As shown in Ref.[10], the proper setting of the single parameter η_{12} to 0.5 allows the model to reproduce with good accuracy the accommodation coefficients[3] of normal and tangential momentum as well as the energy accommodation coefficients computed by MD simulation of the $Xe-Pt$ system.

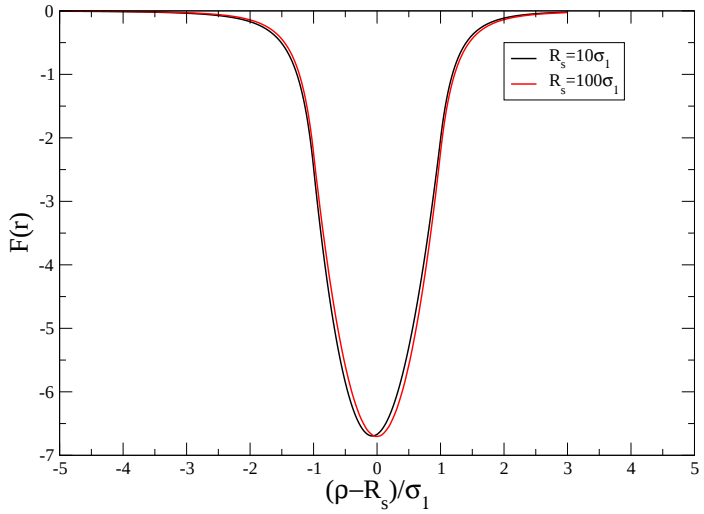

Figure 1: Normalized radial force field profiles in the vicinity of the density step. $Xe - Pt$ system: $\eta_w = 0.7$, $\overline{\phi}^{(12)}/k_B T_{ref} = 1.064$, $\gamma^{(12)} = 6$.

3.1 Flow geometry

The free molecular flow of Xe past a Pt sphere has been simulated by solving the steady kinetic equation

$$\boldsymbol{v}_1 \circ \nabla_{\boldsymbol{r}_1} f_1 + \frac{\boldsymbol{F}_{12}}{m_1} \circ \nabla_{\boldsymbol{v}_1} f_1 = C_{12}(f_1, f_w) \tag{9}$$

It is assumed that the sphere is kept at rest in a reference frame whose origin coincides with the sphere center. The centers of platinum atoms occupy the region $\|\boldsymbol{r}_2\| \leq R_s$ and the local density of the solid is assigned as follows:

$$n_w(\boldsymbol{r}_2) = \begin{cases} \overline{n}_w & \boldsymbol{r}_2 \leq R_s \\ 0 & \boldsymbol{r}_2 > R_s \end{cases} \tag{10}$$

being $\overline{n}_w$ the constant value of the assumed platinum density and R_s the nominal sphere radius. It is further assumed that the temperature of the solid, T_w, is uniform and constant. All the computations have been performed by setting $T_w/T_{ref} = 1$. The above setting completely specify the solid atoms distribution function f_w which takes the form of a Maxwellian having density $n_w(\boldsymbol{r}_2)$, temperature T_w and bulk velocity $\boldsymbol{u}_w = 0$. The mean field associated with the soft attractive tail is also completely specified by substituting Eq.(10) into Eq.(6). The adoption of cylindrical coordinates allows reducing the volume integration at the r.h.s. of Eq.(6) to a one-dimensional integral which can be easily computed by standard quadrature formulas. Radial force field profiles are given in Fig. 1 for $R_s = 10\sigma 1$ and $R_s = 100\sigma_1$; force values are normalized to $k_B T_{ref}/\sigma_1$. As shown in Fig. 1, the radial force field is not much affected by R_s, it has a minimum very close to the density step located at $\rho = R_s$ and rapidly vanishes away from the density step. It is worth observing that the field vanishes inside the solid sphere because a test gas atom sufficiently far from the density step would be equally attracted by all of the uniformly distributed solid atoms. The mathematical formulation

is completed by the following boundary condition

$$\lim_{\boldsymbol{r}\to\infty} f(\boldsymbol{r},\boldsymbol{v}) = f_\infty = \frac{n_\infty}{[2\pi R_1 T_\infty]^{3/2}} \exp\left\{-\frac{(\boldsymbol{v}-\boldsymbol{u}_\infty)^2}{2R_1T_\infty}\right\} \tag{11}$$

which states that the undisturbed gas far from the sphere is in an equilibrium state characterized by density n_∞, temperature T_∞ and bulk velocity $\boldsymbol{u}_\infty$.

3.2 Description of the numerical method

Since molecular interaction in the gas phase is neglected, Eqs.(4,9) are linear. In spite of the simplification, the complex mathematical structure of the term $C_{12}(f_1, f_w)$ makes the adoption of numerical solution methods necessary. Hence, Eq.(9) has been solved by the linear version of the Direct Simulation Monte Carlo (DSMC) method for the solution of the non-linear Enskog equation, described in Ref. [9]. The method is based on the representation of the gas distribution function as an ensemble of N_p mathematical particles characterized by their positions $\boldsymbol{r}_i(t)$ and velocities $\boldsymbol{v}_i(t)$ ($i = 1, \ldots, N_p$). Positions and velocities are advanced from their values at time t to their values at time $t + \Delta t$ by time splitting the evolution operator defined by Eq.(4). Accordingly, position and velocities are updated upon executing two sub-steps. In the first sub-step hard sphere interaction is neglected and the following equation is solved:

$$\frac{\partial f}{\partial t} + \boldsymbol{v} \circ \frac{\partial f}{\partial \boldsymbol{r}} + \frac{\boldsymbol{F}^{(12)}(\boldsymbol{r})}{m_1} \circ \frac{\partial f}{\partial \boldsymbol{v}} = 0 \tag{12}$$

Eq.(12), which describes the phase space motion of a single atom under the action of the mean field $\boldsymbol{F}^{(12)}(\boldsymbol{r})$, can be conveniently discretized by the simple scheme:

$$\boldsymbol{r}_i(t+\Delta t) = \boldsymbol{r}_i(t) + \boldsymbol{v}_i(t)\Delta t + \frac{\boldsymbol{F}^{(12)}(\boldsymbol{r}_i(t))}{m_1}\frac{(\Delta t)^2}{2} \tag{13}$$

$$\boldsymbol{v}_i(t+\Delta t) = \boldsymbol{v}_i(t) + \frac{\boldsymbol{F}^{(12)}(\boldsymbol{r}_i(t))}{m_1}\Delta t \tag{14}$$

In the second sub-step, advection in the phase space is neglected and the following equation is solved:

$$\frac{\partial f}{\partial t} = C^{(12)}(f_w, f) \tag{15}$$

Following Ref.[9], Eq.(15) is solved by a majorant collision frequency scheme. Taking into account that the hard sphere interaction is effective in the spherical domain $\|\boldsymbol{r}\| \le R_s + \sigma_{12}$, a velocity independent upper bound $\overline{\nu}_{coll}(\boldsymbol{r})$ for the real collision frequency $\nu_{coll}(\boldsymbol{r},\boldsymbol{v})$ is constructed from the term $C^{(12)}(f_w, f)$, as follows:

$$\overline{\nu}_{coll}(\boldsymbol{r}) = \begin{cases} 4\pi\sigma_{12}^2 n_w \chi^{(12)}(n_w) V_{max} & \boldsymbol{r} \le R_s + \sigma_{12} \\ 0 & \boldsymbol{r} > R_s + \sigma_{12} \end{cases} \tag{16}$$

being V_max an upper bound for the modulus of the relative velocity $\boldsymbol{v} - \boldsymbol{v}_1$. An upper bound $\overline{P}_{coll}(\boldsymbol{r})$ for the probability $P_{coll}(\boldsymbol{r},\boldsymbol{v})$ that a gas molecule collides with a solid molecule in the time interval $(t, t + \Delta t)$ is easily obtained as $\overline{P}_{coll}(\boldsymbol{r}) = \overline{\nu}_{coll}(\boldsymbol{r})\Delta t$. Since $\overline{P}_{coll}(\boldsymbol{r})$ is larger than the real collision probability, it represents the probability that a gas molecule will suffer either a real or false "collision" which leaves the velocities of colliding atoms unchanged. It is easily shown that

$P_{coll}(\boldsymbol{r},\boldsymbol{v})/\overline{P}_{coll}(\boldsymbol{r}) = (\hat{\boldsymbol{k}}\circ\boldsymbol{v}_r)^+/V_{max}$, hence the collision algorithm runs as follows: each gas atom is considered for a collision (either false or real) with probability $\overline{P}_{coll}(\boldsymbol{r})$, if it "collides", then a random unit vector $\hat{\boldsymbol{k}}$ is generated and a solid molecule position $\boldsymbol{r}-\sigma_{12}\hat{\boldsymbol{k}}$ is obtained. If $\|\boldsymbol{r}-\sigma_{12}\hat{\boldsymbol{k}}\|\leq R_s$ then a solid molecule velocity $\boldsymbol{v}_1$ is drawn from the probability density $\frac{f_w}{n_w}$ and the collision is accepted as a real one with probability $(\hat{\boldsymbol{k}}\circ\boldsymbol{v}_r)^+/V_{max}$. In this case, a new velocity $\boldsymbol{v}^*$ is assigned as to the gas velocity according to the hard sphere collision dynamics:

$$\boldsymbol{v}^* = \boldsymbol{v} + 2\frac{m_2}{m_1+m_2}(\hat{\boldsymbol{k}}\circ\boldsymbol{v}_r)\hat{\boldsymbol{k}} \tag{17}$$

In all other cases, the velocity remains unchanged.
The numerical solution of Eq.(9) is accomplished by applying the scheme depicted above. More precisely, a cut-off distance R_c is defined beyond which the mean field can be safely neglected and the kinetic equation is solved in a cube of side $2R_c$, centered on the origin. N_p particles are injected into the cubic domain at constant rate in the time interval $(0,T_{max})$; their initial positions belong to the cube faces and their initial velocities are drawn from f_∞. The trajectory of each particle inside the cubic domain is computed executing a sequence of the phase space advection and collision substeps. The force on the spherical particle in computed from the expression:

$$\boldsymbol{F}_s = \frac{1}{T_{max}}\sum_{i=1}^{N_p}(\boldsymbol{Q}_i^{(in)} - \boldsymbol{Q}_i^{(out)}) \tag{18}$$

In Eq.(18), $\boldsymbol{Q}_i^{(in)}$ is the value of the $i-th$ gas atom momentum when it enters the spherical volume of radius R_c, $i.e.$ when interaction with the spherical particle starts, whereas $\boldsymbol{Q}_i^{(out)}$ the momentum when the gas atoms exits the spherical volume of radius R_c, $i.e.$ when interaction with the spherical particle stops.

3.3 Description of numerical results

Numerical simulations of the free molecular gas flow past a sphere have been performed for four values of the nominal sphere radius: $R_s = 10\sigma_1, 20\sigma_1, 50\sigma_1, 100\sigma_1$. For each value of R_s, the low Mach number region has been explored by varying $M_\infty = u_\infty/\sqrt{5R_1T_\infty/3}$ from 0.05 to 0.25 in steps of 0.05. The determination of the cut-off distance is a delicate task since the value of the effective sphere radius, which takes into account the attractive tail above the nominal spherical surface, is a key quantity in the calculation of the drag coefficient C_D. The cut-off radius R_c has been determined, for each value of M_∞ and R_s, by computing the force values $\boldsymbol{F}_s$ obtained truncating the effects of the mean field at increasing distance from the nominal surface at R_s. The computations show that the force increases until a critical value of R_c is reached beyond which $\boldsymbol{F}_s$ stabilizes. Any further increase of the truncation radius will not affect $\boldsymbol{F}_s$ because the mean field value is too small to affect the gas motion. The critical value has been found fairly insensitive to M_∞ and R_s in the explored parameters range and very close to $R_s+3\sigma_1$. Accordingly, the sphere drag coefficient C_D has been computed as

$$C_D = \frac{F_s}{\frac{1}{2}m_1 n_\infty u_\infty^2 \pi (R_s+3\sigma_1)^2} \tag{19}$$

being F_s the force component parallel to the downstream velocity.

The computed values of drag coefficients are shown in Fig. 2. Each point has been obtained by a computer run in which about 10^6 trajectories are computed. Each run takes about 5 minutes on

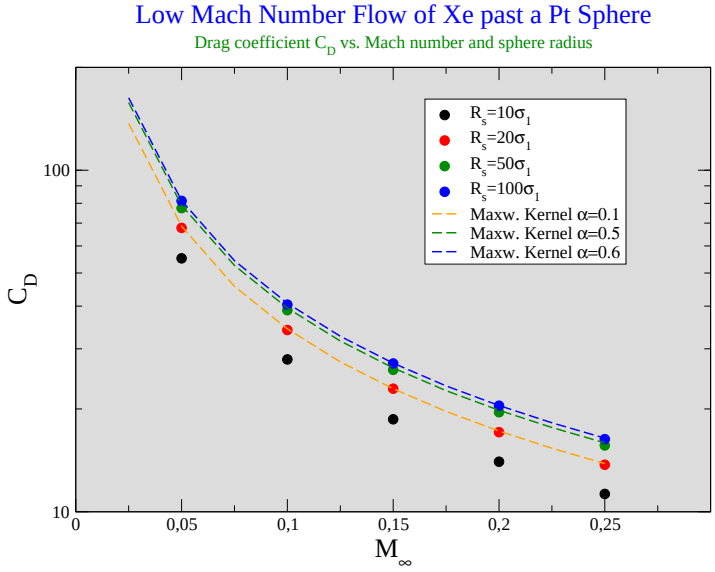

Figure 2: Drag coefficients vs M_∞ and R_s. $Xe - Pt$ system: $\eta_w = 0.7$, $\overline{\phi}^{(12)}/k_B T_{ref} = 1.064$, $\gamma^{(12)} = 6$, $\eta_{12} = 0.5$.

a standard personal computer equipped with a $2.2GHz$ dual core CPU. The percentage statistical error amounts to about 1%. It is to be observed that, for any fixed Mach number value, the drag coefficient is affected by the sphere radius. More precisely, the drag coefficient grows increasing R_s. However, the growth rate is higher in the range $10\sigma_1 \leq R_s \leq 50\sigma_1$, being the drag coefficient difference between the cases $R_s = 50\sigma_1$ and $R_s = 100\sigma_1$ small. Hence, Fig. 2 shows that, for the considered gas-solid interaction parameters setting, spheres of radius larger than $R_s = 100\sigma_1$ will exhibit the familiar behavior, in which momentum accommodation does not depend on radius. Fig. 2 also presents a comparison with the sphere drag coefficient values computed from Eq.(2) varying the accommodation coefficient α. It is to be observed that, for fixed radius R_s, it is possible to determine an effective value of the accommodation coefficient $\alpha_{eff}(R_s)$ which allows Maxwell's model to agree with the kinetic model data. The only exception is represented by the case $R_s = 10\sigma_1$ which fall below the pure specular reflection scattering ($\alpha = 0$). An explanation for the behavior described above can be given by considering in greater detail the motion of gas molecules interacting with the solid sphere. The truncation of the radial force field to R_c makes the total sphere crossection equal to $S_T = \pi R_c^2$. It is convenient to divide the circular crossection area into the sum of an inner circle of radius $R_{in} = R_s + \sigma_{12}$ and area $S_{in} = \pi R_{in}^2$ and an outer ring, delimited by the two radii R_{in} and R_c, whose area is $S_{out} = \pi(R_c^2 - R_{in}^2)$. Let us also define the impact parameter b of a gas molecule as its minimal distance from the sphere center in the uniform rectilinear motion in absence of interactions. It is clear that a gas molecule will "miss" the sphere if $b > R_c$ and it will not contribute to C_D. Those gas molecules which are going to exchange momentum with the sphere can be divided into two groups. The first group is composed by the molecules for which the condition $R_{in} \leq b \leq R_c$ holds. The unperturbed trajectories of these molecules will intersect the outer ring, hence they will be deflected by the radial field and they may either describe a smooth trajectory around the sphere, or suffer short range collisions if deflection exceeds a certain threshold.

The second group is composed by the molecules for which the condition $b < R_{in}$ holds. The initial velocities of these molecules aims at the inner circle, therefore they will certainly experience hard sphere collisions in addition to the action of the radial mean field. Since impacting molecules are evenly distributed in space, the fraction of group one trajectories will be S_{out}/S_T whereas S_{in}/S_T will be the fraction of trajectories in group two. In complete analogy with the overall drag coefficient given by Eq.(19), it is possible to define partial drag coefficients C_D^{in} and C_D^{out} to measure the momentum transfer efficiencies of the two trajectory groups. The definition is straightforward:

$$C_D^{in} = \frac{F_s^{in}}{\frac{1}{2} m_1 n_\infty u_\infty^2 S_{in}} \qquad C_D^{out} = \frac{F_s^{out}}{\frac{1}{2} m_1 n_\infty u_\infty^2 S_{out}} \tag{20}$$

The overall drag coefficient can be rewritten as

$$C_D = C_D^{in} \frac{S_{in}}{S_T} + C_D^{out} \frac{S_{out}}{S_T} \tag{21}$$

The behavior of partial drag coefficients C_D^{in} and C_D^{out} is shown in Fig. 3. As expected, the contri-

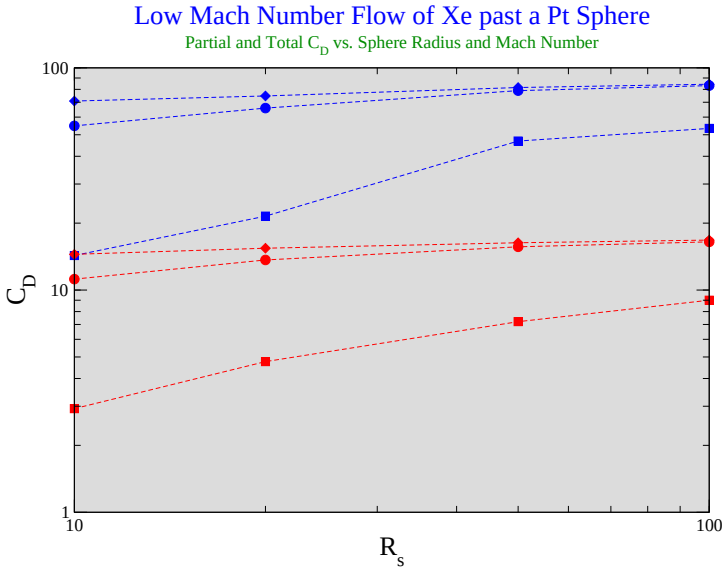

Figure 3: Partial and total C_D vs. R_s for $M_\infty = 0.05$ (blue) and $M_\infty = 0.25$ (red). Filled circles: C_D; filled diamonds: $C_D^{(in)}$; filled squares: $C_D^{(out)}$

bution of C_D^{out} is smaller than C_D^{in} because trajectories in group one are less efficient in transferring momentum from gas to solid. However, C_D^{out} grows with sphere radius because a growing number of trajectories will fall onto the surface. The contribution of C_D^{in} is obviously higher since short range interaction transfers gas momentum more efficiently to the sphere. The behavior of the total drag C_D can now be explained by observing that it results from a linear combination of C_D^{in} and C_D^{out} with weights $\frac{S_{in}}{S_T}$ and $\frac{S_{out}}{S_T}$. At low values of R_s, the weight $\frac{S_{out}}{S_T}$ is not negligible and the lower contribution of C_D^{out} affects the overall drag coefficient. At higher values of R_s the weight

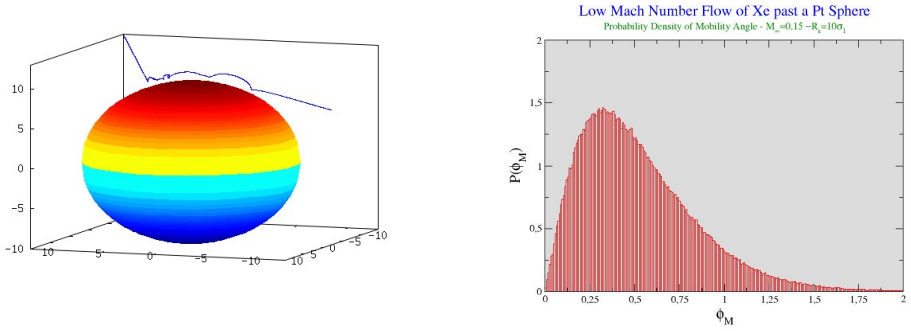

Figure 4: (a) Trajectory of a single Xe atom interacting with a Pt sphere, $R_s = 10\sigma_1$.(b) Mobility angle distribution function,$R_s = 10\sigma_1$

$\frac{S_{out}}{S_T}$ becomes very small and as shown in Fig. 3 C_D practically coincides with C_D^{in}.
Although not immediately evident from Fig. 3, direct inspection of raw data shows that C_D^{in} is a slowly growing function in the range $10\sigma_1 \leq R_s \leq 50\sigma_1$ and becomes constant for $R_s > 50\sigma_1$. A possible explanation is represented by non-local scattering caused by surface diffusion. Fig. 4(a) shows the trajectory of a single atom interacting with the sphere. The atom enters the cubic domain from the upper corner. After the first hard sphere collisions, it bounces a few times till it receives enough energy to escape the mean field attractive action. The reemission position of a molecule can be a few nominal molecular diameters away from the first impact location. A measure of surface mobility, normalized to sphere radius, is given by the angle ϕ_M formed by the gas molecule position vectors on entering and leaving the interaction sphere of radius R_c. As shown in Fig. 4(b), if R_s is of the order of $10\sigma_1$ and the mean displacement during interaction is of the order of a few σ_1's then ϕ_M is relatively large. Since, the molecule has almost forgotten it initial velocity after a few collisions, the reemission velocity direction will be randomly distributed around the local normal vector. If ϕ_M is large, the alignment of initial and reemission velocities is favored and drag is reduced.

4 CONCLUSIONS

The aerodynamics forces in the free molecular flow of a gas around a nanosized particle has been studied by a kinetic model which provides a simplified description of a gas molecule dynamics near a solid surface. The drag coefficients have been computed in the low Mach number region as a function of particle radius. The result confirm the conjecture that momentum accommodation is affected by particle radius R_s and that the drag coefficient is a decreasing function of R_s when the nominal sphere radius has the size of the distance a gas molecule covers on the solid surface between absorption and desorption events. Although the mechanisms responsible for the observed behavior are rather general, more extensive computations are necessary to better understand the response of the results to changes of model physical parameters before a sound comparison with experimental data can be done.

References

[1] Przekop, R., Gradon, L., "Deposition And Filtration Of Nanoparticles In The Composites Of Nano- And Microsized Fibers", *Aerosol Sci. Technol.* **42**(6), 483-493 (2008).

[2] Thimsen, E., Rastgar, N., Biswas, P., "Nanostructured TiO2 Films With Controlled Morphology Synthesized In A Single Step Process: Performance Of Dye-Sensitized Solar Cells And Photo Watersplitting", *Journal Of Physical Chemistry C* **112**(11), 4134-4140 (2008).

[3] C. Cercignani, *The Boltzmann Equation and Its Applications*, Springer-Verlag, Berlin (1988).

[4] Tammet, H., "Size And Mobility Of Nanometer Particles,Clusters And Ions", *J. Aerosol Sci.* **26**(3), 459-475 (1995).

[5] Li Z., Wang, H., "Drag Force, Diffusion Coefficient and Electric Mobility of Small Particles...", Phys. Rev. E **68**, 061206 (2003).

[6] Kilpatrick, W. D., "An Experimental Mass-Mobility Relation For Ions In Air At Atmospheric Pressure", *Proc. 19th Annu. Conf. Mass Spectrosc.*, 320-325 (1971).

[7] Li Z., Wang, H., "Gas-Nanoparticle Scattering: A Molecular View of Momentum Acommodation Function", PRL **95**, 014502 (2005).

[8] A. Frezzotti, L. Gibelli, "A Kinetic Model for Fluid-Wall Interaction", Journal of Mechanical Engineering Science, **222** 787-795 (2008).

[9] Frezzotti, A., "A particle scheme for the numerical solution of the Enskog equation", Phys. Fluids **9**, 1329-1335 (1997).

[10] Frezzotti A., Nedea S.V., Markvoort A.J., Spijker P., Gibelli L., "Comparison of Molecular Dynamics and Kinetic Modelling of Gas-Surface Interactions", *Proc. XXVI International Symposium on Rarefied Gas Dynamics* (AIP Conference Proceedings vol. 1084, New York, 2009) Kyoto, Japan, July 21-26 2008, 635-640 (2009).

[11] N.F. Carnahan and K.E. Starling, "Equation of state for nonactracting rigid spheres", *J. Chem. Phys.* **51**, 635 (1969).